Laser Beam Combining in Potassium Vapor

Mark T. Gruneisen, Kenneth R. MacDonald, Alexander L. Gaeta, Robert W. Boyd, *Member, IEEE*, and Donald J. Harter

Abstract—**We have investigated energy transfer between two laser beams of comparable intensity due to their nonlinear interaction in an atomic vapor. Strong coupling occurs due stimulated Rayleigh scattering when the frequencies of the two waves differ by the inverse of the excited-state lifetime. We have measured the energy transfer between two nearly-equal energy pulses from an alexandrite laser tuned near the $4^2S_{1/2} \rightarrow 4^2P_{3/2}$ transition of potassium vapor. As much as 85% of the total incident energy was contained in one of the output beams.**

INTRODUCTION

IN this paper, we investigate the energy coupling that occurs between two laser fields of comparable intensity as they propagate through an atomic vapor. We predict theoretically and verify experimentally that high-coupling efficiencies occur when the two fields are tuned near the atomic resonance and detuned from one another by approximately the inverse of the atomic lifetime. The ability to transfer energy coherently from one laser beam to another could be useful in the generation of extremely intense laser fields.

The interaction of a single intense laser field with a two-level atom modifies the energy-level structure of the atom. This modification can be conveniently described in terms of "dressed" atomic states [1]. Transitions among the dressed states give rise to resonances in the atomic response which can lead to amplification of a weak probe wave. Mollow [2] has calculated the probe-wave absorption spectrum of a collection of strongly driven atoms and predicts three spectral features, two of which can lead to the amplification of the probe wave. One of these gain features occurs when the probe is detuned from the pump wave by the generalized Rabi frequency and is known as stimulated three-photon scattering. The other gain feature occurs when the pump wave is detuned from the pump wave by the inverse of the excited-state lifetime and is a form of stimulated Rayleigh scattering [3]–[9]. Wu *et al.* [10] observed the predicted gain spectrum using a sodium atomic beam as the two-level system. More recently [11], we showed that both the Rabi-sideband and the Rayleigh resonances can give rise to large amplification of a weak probe wave in sodium vapor, where the atomic number density can be much higher than in an atomic beam. In particular, we reported thirty-eightfold and fourfold increases in the probe intensity at the Rabi-sideband and the Rayleigh resonances, respectively, in a 7 mm interaction length. However, with the existence of high gain the weak-probe limit does not guarantee that efficient energy transfer will occur when the intensity of the probe wave is comparable to that of the pump wave.

To treat the energy-transfer characteristics of the nonlinear coupling, one must consider the interaction of a two-level system with *two* strong fields [12]–[17]. Gush and Gush [12] and Tsukada [13] have used continued-fraction techniques to solve the density-matrix equations of motion for the interaction of two strong RF magnetic fields with a two-level system. Bonch-Breuvich *et al.* [14] presented a theory for the case of a pump field tuned exactly to resonance for equal pump-probe intensities. They predicted that resonances will occur in the probe-transmission spectrum whenever the probe-pump detuning is equal to a subharmonic of the Rabi frequency. In addition, they demonstrated that the interaction of strong rf magnetic fields with cadmium vapor agreed with the results of their theory. The existence of subharmonic resonances in the probe-absorption spectrum are also predicted in the interaction of a two-level atom with two electromagnetic fields of arbitrary intensities and frequencies [15], [16]. In addition, Tsukada and Nakayama [15] showed that the Rayleigh resonance is present when the pump field is tuned off resonance. Agarwal and Nayak [17] showed theoretically that the strength of the subharmonic resonances decreases rapidly as the laser bandwidth increases. Experimental studies of the interaction of two intense optical fields with a two-level system have been performed by Hillman *et al.*, [18] and by Chakmakjian *et al.*, [19] who observed subharmonic resonances in the response of a sodium atomic beam driven by a 100%-amplitude-modulated laser field.

In this paper, we investigate the coupling that occurs between two strong waves. When the effects of atomic motion and the spatial variation of the intensities of each wave are taken into account, we find that the Rayleigh resonance can give rise to efficient coupling between two waves of comparable intensity. These predictions were verified experimentally using the output of a pulsed alexandrite laser tuned near resonance in potassium vapor. For the case of equal-input pulse energies, we measured a maximum transfer efficiency that corresponds to one output wave containing as much as 85% of the total incident optical energy.

THEORY

We consider the process in which two monochromatic nearly copropagating laser beams interact with an atomic vapor, as shown in Fig. 1. We allow each beam to be sufficiently intense to saturate the atomic medium. We are interested in determining those conditions under which a significant fraction of the power contained in one beam can be transferred to the other.

The coupled differential equations describing the spatial evolution of the intensities I_1 and I_2 of the two waves are derived

Manuscript received August 8, 1989; revised August 1, 1990. This research was supported in part by the Office of Naval Research under Contract B00014-86-K-0746 and by the sponsors of the New York State Center for Advanced Optical Technology.

M. T. Gruneisen, K. R. MacDonald, A. L. Gaeta, and R. W. Boyd are with the Institute of Optics, University of Rochester, Rochester, NY 14627.

D. J. Harter is with Allied-Signal, Inc., Morristown, NJ 07960.

IEEE Log Number 9041011.

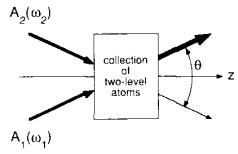

Fig. 1. Interaction geometry. Two optical fields with amplitudes A_1 and A_2 cross at an angle θ in a vapor of two-level atoms. The frequencies ω_1 and ω_2 of the fields are nearly resonant with the atomic transition frequency ω_0.

in the Appendix and have the form

$$\frac{dI_j}{dz'} = -\alpha_j(I_1, I_2)I_j \qquad j = 1, 2 \tag{1}$$

where $z' = z/\cos\theta$, and α_j is the effective absorption coefficients for the jth wave given by

$$\alpha_j(I_1, I_2,) = -N\sigma_0 w_0 \Lambda_j \left\{1 - I_{3-j}\left[\mathrm{Re}(L_1 F) \pm \Delta_j T_2 \mathrm{Im}(L_1 F)\right]\right\} \tag{2}$$

where we take the plus sign for $j = 1$ and the minus sign for $j = 2$. Here F is a continued fraction [(A16)] that depends on the intensities I_1 and I_2, on the detuning $\Delta_j = \omega_j - \omega_0$ of the jth wave from the atomic resonance ω_0, and on material parameters such as the saturation intensity I_s and the relaxation times T_1 and T_2. The quantities Λ_j and L_1 are detuning factors, N is the atomic number density, σ_0 is the line-center intensity absorption cross section, and w_0 is the spatially-averaged steady-state population inversion in the presence of the two waves. For convenience, we denote the waves with intensities I_1 and I_2 as the pump and probe waves, respectively.

In Fig. 2, the effective probe-wave absorption coefficient α_2, given by (2), is plotted as a function of the probe-pump detuning $\delta = \omega_2 - \omega_1$ for several values of the probe–pump intensity ratio. The pump intensity I_1 is taken to be equal to 5×10^3 times the saturation intensity, the pump detuning from resonance Δ_1 is given by $\Delta_1 T_1 = -25$, and the transition is assumed to be radiatively broadened ($T_2/T_1 = 2$). In Fig. 2(a), the probe intensity is much smaller than both the pump intensity and the saturation intensity. The two dominant spectral features occur at the Rabi sidebands, that is, for $\delta = \pm\Omega'$ where the generalized Rabi frequency is given by $\Omega' \equiv (\Delta^2 + \Omega^2)^{1/2}$, where $\Omega \equiv |\mu| E_1/\hbar$ is the on-resonance Rabi frequency, μ is the matrix element of the atomic-dipole operator between the ground and excited states, and E_1 is the (real) amplitude of the pump field. In this figure, the Rayleigh resonance (near $\delta = 0$) is barely visible on the scale chosen to display the Rabi-sideband resonances. In this limit, the absorption spectrum is identical to that predicted by solving the density-matrix equations of motion to first order in the probe-field amplitude [4], [11]. When the probe intensity I_2 is much greater than the saturation intensity, but only a few percent of the pump intensity I_1 [Fig. 2(b)], new resonances in the probe-transmission spectrum appear when the probe-pump detuning is a subharmonic of the generalized Rabi frequency. The principal consequences of increasing the probe intensity are to reduce the amplitudes of the Rabi resonances and to broaden them. In the case shown here, the Rabi resonances and the Rayleigh resonance have comparable amplitudes, because the latter is relatively insensitive to probe intensity. When the probe and pump intensities are equal [Fig. 2(c)], there are a large number of subharmonic resonances and the Rayleigh resonance has a larger amplitude than any of the Rabi-subharmonic resonances.

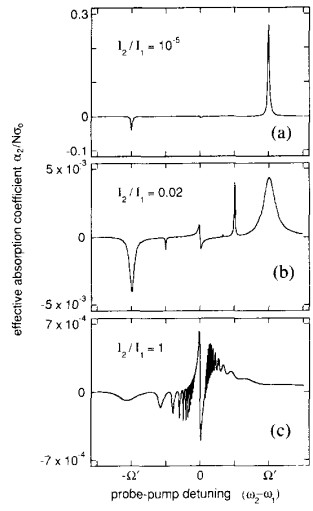

Fig. 2. Effective probe-wave absorption coefficient plotted against the probe-pump detuning for several different values of the probe-pump intensity ratio. The pump intensity I_1 is $5 \times 10^3 I_s$, the pump detuning from resonance is $\Delta_1 T_1 = -25$, and the transition is assumed to be radiatively broadened ($T_2/T_1 = 2$). (a) When the probe intensity is much lower than both the pump intensity and the saturation intensity, the spectrum consists of three features: gain at one (the leftmost) Rabi sideband, gain at the Rayleigh resonance, which is centered on the pump frequency and is barely visible on this scale, and strong absorption at the other Rabi sideband. (b) When the probe intensity is much higher than the saturation intensity, but still lower than the pump intensity, new resonances appear at subharmonics of the generalized Rabi frequency. (c) When the pump and probe intensities are equal, a large number of resonances at subharmonics of the generalized Rabi frequency appear. The insensitivity of the Rayleigh resonance to increased probe intensity makes it the strongest resonance in the spectrum for this case.

The effects of atomic motion are illustrated for the case of copropagating waves in Fig. 3. In Fig. 3(a), the homogeneously-broadened absorption coefficient α_2 [(4)] is evaluated as a function of the normalized probe-pump detuning δT_1 for the case of equal-input intensities, radiative broadening, a total-input intensity equal to $1 \times 10^6 I_s$, and a normalized detuning from resonance of $\Delta_1 T_1 = -500$. The scaling of the horizontal axis was chosen to show clearly the structure of the subharmonic resonances near zero relative detuning. In Fig. 3(b), the effective-absorption coefficient shown in Fig. 3(a) is averaged over a Maxwellian distribution of atomic velocities. The Doppler width is taken to be 200 natural linewidths. Doppler averaging severely reduces the amplitudes of the subharmonic resonances because the generalized Rabi frequency depends on atomic velocity through Doppler shifts in the pump detuning from resonance Δ_1. Consequently, the position of the Rabi resonances is different for each velocity group. In contrast, the Rayleigh-resonance line shape is relatively insensitive to the pump detuning from resonance Δ_1, but depends strongly on the probe-pump detuning δ measured in the reference frame of the atom. Therefore, since the probe-pump detuning is independent of atomic velocity for copropagating beams, the Rayleigh resonance is not broadened by atomic motion.

The effects of propagation are included by integrating (1) numerically. We define the power-transfer efficiency as the fraction of the total incident power that is contained in one of the

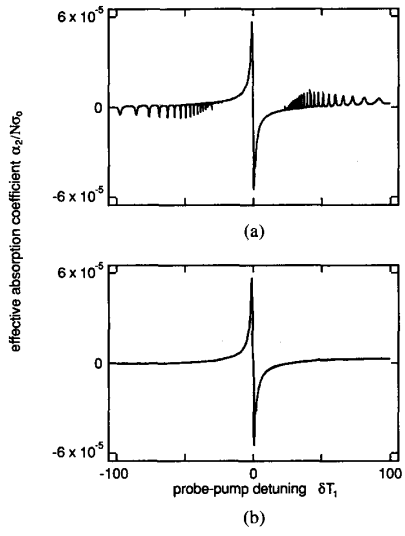

Fig. 3. Effective absorption coefficient for the probe beam plotted against the probe-pump detuning without (a) and with (b) Doppler broadening. We have assumed equal-input intensities, radiative broadening, a total-input intensity $I_{\text{total}}(0) = 1 \times 10^6 I_s$, and a normalized detuning from resonance of $\Delta_1 T_1 = -500$. In (b), the effective absorption coefficient is averaged over a Maxwellian distribution of atomic velocities appropriate for a vapor of potassium atoms at 250°C. Atomic motion completely washes out the resonances near the Rabi subharmonic frequencies, but does not affect the Rayleigh resonance.

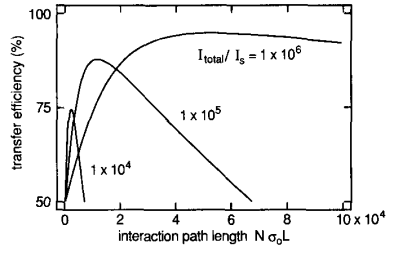

Fig. 4. The transfer efficiency at the peak of the Rayleigh resonance plotted against the interaction path length $N\sigma_0 L$ for various values of the total-incident intensity. The input waves have equal intensities and the transition is radiatively broadened ($T_2/T_1 = 2$). As the incident intensity increases, the maximum coupling increases and occurs for a larger interaction path length. Note that transfer efficiencies as high as 95% are predicted. For each value of the incident intensity, the laser detuning from resonance is taken to be equal to one-half of the Rabi frequency for one of the input waves, which we have found from numerical calculations to be nearly the optimum value.

output waves. In Fig. 4, the power-transfer efficiency, evaluated at the peak of the Rayleigh resonance, is plotted as a function of interaction path length $N\sigma_0 L$ for various values of the total-input intensity. We assume the case of equal-input intensities, radiative broadening, and copropagating waves. For each plot the detuning of the pump wave from resonance Δ_1 is taken to be one-half of the Rabi frequency Ω associated with one input wave. We have observed from our computer calculations that this detuning is nearly optimal. This detuning is nearly optimal because it corresponds to the best compromise between enhancement of the nonlinearity which occurs near resonance and decreased absorption which occurs far from resonance. As the total input intensity increases, the maximum-power transfer efficiency increases and occurs at a higher value of $N\sigma_0 L$. Note that the calculated coupling efficiency is ~95% when the total-input intensity is equal to $1 \times 10^6 I_s$ and the absorption path length is $\sim 5 \times 10^4$.

Experiment

The experimental setup is illustrated schematically in Fig. 5. A pulsed alexandrite laser [20] was tuned near resonance with the potassium $4^2S_{1/2} \rightarrow 4^2P_{3/2}$ transition using a four-plate birefringent filter and a 1 mm thick étalon. The detuning of the laser frequency from resonance was monitored using a 3/4-meter Czerny–Turner spectrometer in conjunction with a linear detector array and optical multichannel analyzer. The spectrometer provided a resolution of 0.03 Å and was calibrated through the use of a potassium arc lamp. The output spectrum of the laser typically consisted of two longitudinal modes. The data in Figs. 6–7 were measured with the laser free running; the data shown in Fig. 8 were obtained with a Q-switched oscillator, so that each data pair represents the energy coupling experienced by a single laser pulse. The temporal output of the free-running laser consisted of a train of 2–5 pulses, each approximately 1 μs in duration and having an average pulse energy of about 150 μJ. When the alexandrite laser was Q switched, it produced a single output pulse of 500 ns duration and an average energy of about 150 μJ. The corresponding peak laser intensity at the potassium cell was approximately 2×10^6 times the line-center saturation intensity (2.8 mW/cm^2) for this transition in potassium.

In order to produce two beams with the necessary relative frequency detuning, the laser output was passed through two variable-frequency traveling-wave acoustooptic modulators. Since each modulator can be tuned over a 40 MHz range about its nominal operating frequency of 80 MHz, this arrangement allowed us to vary the relative detuning of the two diffracted beams over a range that was much larger than the 3 MHz width of the Rayleigh resonance. The first-order-diffracted components from the acoustooptic modulators were brought together in a 7 mm long potassium-vapor cell consisting of a stainless-steel body and sidearm. The sidearm temperature was typically between 200 and 250°C, corresponding to a potassium number density of 10^{14}–10^{15} atoms/cm^3. Polarization distortions were minimized by using zero-degree-oriented sapphire windows at near-normal incidence.

We observed experimentally that the measured transfer efficiency depends critically upon the crossing angle of the beams in the potassium cell. The strength of the Rayleigh resonance is known theoretically to be largest for a zero beam-crossing angle, and decreases rapidly with increasing crossing angle due to the effects of atomic motion [11]. However, at small crossing angles, Raman–Nath scattering [21] into higher orders causes a substantial loss of energy from the two transmitted beams. We have determined experimentally that the smallest crossing angle for which Raman–Nath scattering did not significantly degrade the coupling efficiency was ~0.6°.

The total-peak intensity incident on the cell was varied from 1 W/cm^2 to 40 kW/cm^2 with a variable attenuator consisting of a rotatable half-wave plate and a linear polarizer. The integrated energy of each transmitted beam, as well as the total-input energy, was recorded for each laser shot using large-area photodiodes, an analog-to-digital converter, and a laboratory computer. The energy-transfer efficiency measured in the experiments is defined as the fraction of the total-incident pulse energy contained in one of the output pulses. All of the data in Figs. 6–8 were obtained using input pulses of equal energy.

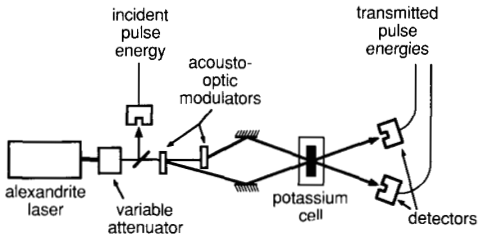

Fig. 5. Experimental setup. The output of a pulsed alexandrite laser is split into two beams with variable frequencies by a pair of independently controllable acoustooptic modulators. The two beams intersect in a cell containing a vapor of potassium atoms. The transmitted energies of the beams are monitored with large-area integrating detectors.

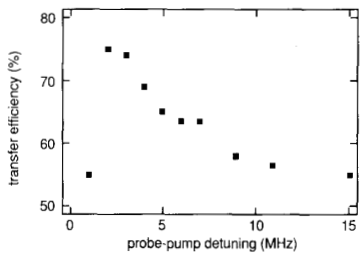

Fig. 6. Energy transfer efficiency plotted against the relative detuning of the two input beams. The detuning of the pump beam from the atomic resonance frequency was −21 GHz, and the incident pulses had equal energy.

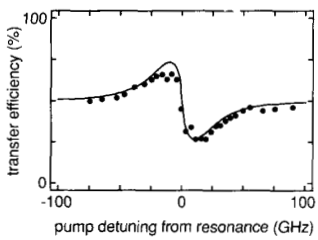

Fig. 7. Dependence of the energy transfer efficiency on the pump detuning from resonance. The probe-pump detuning was fixed at 3 MHz to optimize the coupling efficiency. The solid curve shows the predictions of the theory described in the text.

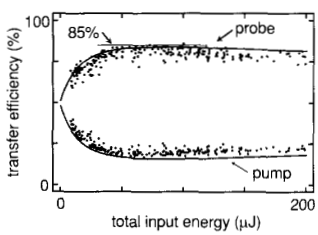

Fig. 8. Fraction of the total-input energy leaving in each of the output beams plotted against the total-input energy. The probe-pump detuning was 3 MHz, and the laser was detuned from resonance by −38 GHz. For a total input energy of ~75 μJ, as much as 85% of the total incident energy was contained in one of the output beams. The solid curve shows the predictions of theory.

The dependence of the energy-transfer efficiency on the relative detuning of the two input beams is plotted in Fig. 6. Each data point was obtained by setting the frequency of one of the acousticooptic modulators to provide the desired relative detuning, and then realigning the two beams to compensate for the small resulting angular misalignment. The pump was detuned from the stationary-atom resonance frequency by −21 GHz (that is, 21 GHz toward the red end of the spectrum) and each pulse contained 20 μJ of energy. The body of the vapor-cell was held at a temperature of ~220°C. The maximum coupling efficiency occurred when the frequency of the pump beam was ~3 MHz.

In Fig. 7, we show the dependence of the coupling efficiency on the detuning of the laser from the atomic-resonance frequency. The probe-pump detuning was 3 MHz, which optimizes the coupling efficiency as observed in Fig. 6. These data were obtained with each input pulse containing 20 μJ of energy.

The fraction of the total input energy contained in each transmitted beam is plotted in Fig. 8 *versus* the total-incident energy. The two beams were detuned from each other by 3 MHz, the laser was detuned from the atomic resonance by −38 GHz. Note that for total-input pulse energies on the order of 100 μJ, as much as 85% of the total-incident energy was contained in one of the transmitted beams. The solid lines shown in Figs. 7 and 8 are theoretical predictions obtained by numerically integrating the coupled-intensity equations (1) for conditions similar to those of our experimental study. We take the laser spot size within the atomic vapor and the temperature of the atomic vapor to be free parameters in our numerical analysis. We found that to obtain a good fit to the data, the laser intensity inside the cell was assumed to be six times larger (i.e., a 0.4 mm beam diameter) than the measured value, and the vapor temperature was 45°C lower (175°C for Fig. 7 and 205°C for Fig. 8) than the value measured at the sidearm. The discrepancies between the values of the intensity could be explained by the fact that in the theory we assumed monochromatic plain waves for the laser beams, whereas the experimental beams would be more accurately described by Gaussian temporal and spatial profiles. The discrepancy between the values for the vapor temperature could be due to optical pumping effects, which would decrease the effective number density, or due to temperature gradients within the cell.

Discussion

The largest measured coupling efficiency of ~85% (Fig. 8) represents a substantial energy transfer from one laser beam to the other. However, the theoretical results shown in Fig. 4 suggest that a transfer efficiency of ~95% should have been observed within the range of conditions accessible in our experiment. This mild disagreement can be attributed to the finite spatial and temporal extent of the laser beams used in the experiment. Some loss of efficiency occurs as a result of the weak coupling between the less intense parts of the pulses.

Finally, the interpretation of the experimental situation is complicated by the unavoidable presence of self-focusing and defocusing. On the self-focusing side of resonance, we were not able to measure transfer efficiencies as large as those measured on the self-defocusing side of resonance. The breakup of the beams due to self-focusing probably reduces the length over which the beams interact, and hence degrades the transfer efficiency.

Conclusion

We have shown theoretically that the interaction of two intense waves by means of the Rayleigh resonance can result in efficient energy transfer from one wave to the other. We verified this theoretical prediction by investigating the coupling of two

equal-energy laser pulses in potassium vapor. We observed that up to 85% of the total energy in the two input pulses could be contained in one of the output pulses. The results presented here suggest that this interaction may be suitable for laser-beam combining applications.

Appendix

In this Appendix, we derive (1)–(2) for the intensities of two nearly-copropagating plane waves as they interact in a system of two-level atoms. The optical fields are assumed to be linearly polarized along the direction normal to the interaction plane and to have amplitudes A_1 and A_2, frequencies ω_1 and ω_2, and wave vectors $\boldsymbol{k}_1$ and $\boldsymbol{k}_2$, respectively. The total optical field is then written

$$E(\boldsymbol{r}, t) = \left[A_1(\boldsymbol{r}) \exp\left[i(\boldsymbol{k}_1 \cdot \boldsymbol{r} - \omega_1 t)\right] + A_2(\boldsymbol{r}) \exp\left[i(\boldsymbol{k}_2 \cdot \boldsymbol{r} - \omega_2 t)\right]\right] + \text{c.c.} \quad \text{(A1)}$$

The interaction of a single stationary atom with the two optical fields is described by the equations of motion for the elements of the density matrix [22]

$$\frac{d\rho_{\text{ba}}}{dt} = -(i\omega_0 + 1/T_2)\rho_{\text{ba}} + i\frac{V_{\text{ba}}}{\hbar} w \quad \text{(A2)}$$

$$\frac{dw}{dt} = -\frac{1}{T_1}(w - w_{\text{eq}}) + \frac{2i}{\hbar}\left[V_{\text{ab}}\rho_{\text{ba}} - V_{\text{ba}}\rho_{\text{ab}}\right] \quad \text{(A3)}$$

where ρ_{ba} describes the coherence between atomic states $|a>$ and $|b>$, $w = \rho_{bb} - \rho_{aa}$ is the atomic inversion, w_{eq} is the steady-state population inversion in the absence of applied fields which we take to be equal to -1, T_2 is the dipole-dephasing time, T_1 is the population relaxation time, and ω_0 is the atomic-resonance frequency. In the rotating-wave approximation, the atom-field interaction energy V_{ab} is given by

$$V_{ba}(\boldsymbol{r}, t) = -\mu\left[A_1(\boldsymbol{r}) \exp\left[i(\boldsymbol{k}_1 \cdot \boldsymbol{r} - \omega_1 t)\right] + A_2(\boldsymbol{r}) \exp\left[i(\boldsymbol{k}_2 \cdot \boldsymbol{r} - \omega_2 t)\right]\right]. \quad \text{(A4)}$$

In order to solve (A2) and (A3), we introduce the following Floquet expansions for ρ_{ba} and w:

$$\rho_{ba}(\boldsymbol{r}, t) = \left[\sum_{n=-\infty}^{\infty} d_n \exp\left[in\left[(\boldsymbol{k}_2 - \boldsymbol{k}_1) \cdot \boldsymbol{r} - \delta t\right]\right]\right] \cdot \exp\left[i(\boldsymbol{k}_1 \cdot \boldsymbol{r} - \omega_1 t)\right] \quad \text{(A5)}$$

$$w(\boldsymbol{r}, t) = \sum_{n=-\infty}^{\infty} w_n \exp\left[in\left[(\boldsymbol{k}_2 - \boldsymbol{k}_1) \cdot \boldsymbol{r} - \delta t\right]\right] \cdot (w_{-n} = w_n^*) \quad \text{(A6)}$$

where $\delta = \omega_2 - \omega_1$. After substituting (A5)–(A6) into (A2)–(A3), the coefficients of those terms having the same frequency dependence are equated, giving

$$in\delta d_n = -(i\Delta_1 - 1/T_2)d_n + i\frac{\mu}{\hbar}\left[A_1 w_n + A_2 w_{n-1}\right] \quad \text{(A7)}$$

$$in\delta w_n = \frac{2i}{\hbar}\left[\mu(d_n A_1^* + d_{n+1}A_2^*) - \mu(d_{-n}^* A_1 + d_{-(n-1)}A_2)\right] + \frac{(w_n + \delta_{n0})}{T_1} \quad \text{(A8)}$$

where $\Delta_1 = \omega_1 - \omega_0$ and δ_{ij} is the Kronecker delta. We solve (A7) for d_n and substitute the result into (A8) in order to obtain the following recursion relation for the coefficients w_n:

$$in\delta T_1 w_n = (1 + M_{1n}I_1 + M_{2n}I_2)w_n + L_n I_c w_{n-1} + L_{n+1}I_c^* w_{n+1} + \delta_{n0} \quad \text{(A9)}$$

where

$$L_n = \frac{1}{2I_s}\left\{\frac{1}{1 - i(\Delta_1 + n\delta)T_2} + \frac{1}{1 + i(\Delta_2 - n\delta)T_2}\right\} \quad \text{(A10)}$$

$$M_{jn} = \frac{1}{2I_s}\left[\frac{1}{1 - i(\Delta_j + n\delta)T_2} + \frac{1}{1 + i(\Delta_j - n\delta)T_2}\right] \quad \text{(A11)}$$

$$I_j = \frac{c}{2\pi}|A_j|^2 \qquad j = 1, 2 \quad \text{(A12)}$$

$$I_c = \frac{c}{2\pi}A_1^* A_2 \quad \text{(A13)}$$

where $\Delta_2 = \omega_2 - \omega_0$ and $I_s = c\hbar^2/8\pi|\mu|^2 T_1 T_2$. If we define $R_n \equiv w_n/w_{n-1}$, then, for $n \neq 0$, (A9) can be expressed as

$$R_n = \frac{-L_n I_c}{1 + M_{1n}I_1 + M_{2n}I_2 - in\delta T_1 + L_{n+1}I_c^* R_{n+1}}. \quad \text{(A14)}$$

In order to obtain the terms in the nonlinear polarization that are phase-matched to either of the two incident waves, we must derive explicit expressions for w_0 and w_1. Iterating (A14) yields one relation between w_0 and w_1:

$$\frac{w_1}{w_0} = R_1 = -L_1 I_c F \quad \text{(A15)}$$

where F is the continued fraction

$$F = \cfrac{1}{1 + \Phi_1 - \cfrac{(L_2)^2|I_c|^2}{1 + \Phi_2 - \cfrac{(L_3)^2|I_c|^2}{1 + \Phi_3 - \cfrac{(L_4)^2|I_c|^2}{\ddots}}}} \quad \text{(A16)}$$

and $\Phi_n \equiv M_{1n}I_1 + M_{2n}I_2 - in\delta T_1$. Setting $n = 0$ in (A9) yields a second relation between w_0 and w_1:

$$-(1 + M_{10}I_1 + M_{20}I_2)w_0 = L_0 I_c w_1^* + L_1 I_c^* w_1 + 1. \quad \text{(A17)}$$

Equations (A15)–(A17) can be solved for w_0 and w_1 to give

$$w_0 = \frac{-1}{1 + \Lambda_1 I_1/I_s + \Lambda_2 I_2/I_s - 2|I_c|^2 \operatorname{Re}\left\{(L_1)^2 F\right\}} \quad \text{(A18)}$$

$$w_1 = \frac{L_1 I_c F}{1 + \Lambda_1 I_1/I_s + \Lambda_2 I_2/I_s - 2|I_c|^2 \operatorname{Re}\left\{(L_1)^2 F\right\}} \quad \text{(A19)}$$

where $\Lambda_j = 1/[1 + (\Delta_j T_2)^2]$, $j = 1, 2$. If we retain only those terms in (A5) that are phase matched to either of the two incident waves, the expansion of $\rho_{ba}(r, t)$ becomes

$$\rho_{ba}(\boldsymbol{r}, t) = d_0 \exp\left[i(\boldsymbol{k}_1 \cdot \boldsymbol{r} - \omega_1 t)\right] + d_1 \exp\left[i(\boldsymbol{k}_2 \cdot \boldsymbol{r} - \omega_2 t)\right] \quad \text{(A20)}$$

where

$$d_0 = \frac{\mu T_2}{\hbar} \frac{\Delta_1 T_2 - i}{1 + (\Delta_1 T_2)^2} (A_1 w_0 + A_2 w_1^*) \qquad \text{(A21)}$$

and

$$d_1 = \frac{\mu T_2}{\hbar} \frac{\Delta_2 T_2 - i}{1 + (\Delta_2 T_2)^2} (A_1 w_1 + A_2 w_0). \qquad \text{(A22)}$$

The variation in the amplitudes of the two waves as they propagate through a collection of stationary two-level atoms is described by Maxwell's wave equation:

$$\nabla^2 E(r, t) - \frac{1}{c^2} \frac{\partial^2 E(r, t)}{\partial t^2} = \frac{4\pi}{c^2} \frac{\partial^2 P(r, t)}{\partial t^2} \qquad \text{(A23)}$$

where $P(r, t)$ is the polarization, which is given by

$$P(r, t) \approx N\mu\rho_{ba}(r, t) + \text{c.c.} \qquad \text{(A24)}$$

where N is the atomic number density. By combining (A20)–(A24) and making the slowly-varying-envelope approximation, we obtain the following coupled equations for the slowly-varying field amplitudes:

$$\frac{dA_1}{dz'} = \frac{1}{2}(1 + i\Delta_1 T_2) N\sigma_0 \Lambda_1 (1 - L_1^* F^* I_2) w_0 A_1 \qquad \text{(A25)}$$

$$\frac{dA_2}{dz'} = \frac{1}{2}[1 + i\Delta_2 T_2] N\sigma_0 \Lambda_2 (1 - L_1 F I_1) w_0 A_2. \qquad \text{(A26)}$$

In (A25)–(A26), $z' = z/\cos\theta$, where z is the axis along the bisector of wave vectors $\boldsymbol{k}_1$ and $\boldsymbol{k}_2$ and 2θ is the crossing angle between the waves in the nonlinear medium (Fig. 1), $\sigma_0 = 4\pi |\mu|^2 T_2 \omega_0/\hbar c$ is the weak-field, linecenter intensity absorption cross section. In deriving (A25)–(A26), we have assumed that $\delta \ll \omega_0$ and that the two waves are nearly copropagating in the nonlinear medium ($\sin\theta \ll 1$). The coupled equations (1) and (2) for the intensities of the two waves follow directly from (A25)–(A26).

References

[1] C. Cohen-Tannoudji and S. Reynaud, "Dressed atom description of resonance fluorescence and absorption spectra of a multilevel atom in an intense laser beam," *J. Phys. B*, vol. 10, pp. 345–363, 1977; "Modification of resonance Raman scattering in very intense laser fields," *J. Phys. B*, vol. 10, pp. 365–383, 1977; "Simultaneous saturation of two atomic transitions sharing a common level," *J. Phys. B*, vol. 10, pp. 2311–2331, 1977; E. Courtens and A. Szöke, "Time and spectral resolution in resonance scattering and resonance fluorescence," *Phys. Rev. A*, vol. 15, pp. 1588–1693, 1977; Errata, vol. 17, p. 2119, 1978.

[2] B. R. Mollow, "Stimulated emission and absorption near resonance for driven systems," *Phys. Rev. A*, vol. 5, pp. 2217–2222, 1972.

[3] R. W. Boyd, M. G. Raymer, P. Narum, and D. J. Harter, "Four-wave parametric interactions in a strongly driven two-level system," *Phys. Rev. A*, vol. 24, pp. 411–423, 1981.

[4] M. Sargent III, "Spectroscopic techniques based on Lamb's theory," *Phys. Rep.*, vol. 43, pp. 223–265, 1978.

[5] S. E. Schwartz and T. Y. Tan, "Wave interactions in saturable absorbers," *Appl. Phys. Lett.*, vol. 10, pp. 4–7, 1967.

[6] J. H. Lee, J. J. Song, M. A. F. Scarparo, and M. D. Levenson, "Coherent population oscillations and hole burning observed in Sm^{+2}:CaF_2 using polarization spectroscopy," *Opt. Lett.*, vol. 5, pp. 196–198, 1980.

[7] J. J. Song, J. H. Lee, and M. D. Levenson, "Picosecond relaxation measurements by polarization spectroscopy in condensed phases," *Phys. Rev. A*, vol. 17, pp. 1439–1447, 1978.

[8] L. W. Hillman, R. W. Boyd, J. Krasinski, and C. R. Stroud, Jr., "Observation of a spectral hole due to population oscillations in a homogeneously broadened optical line," *Opt. Commun.*, vol. 45, pp. 416–419, 1983.

[9] M. S. Malcuit, R. W. Boyd, L. W. Hillman, J. Krasinski, and C. R. Stroud, Jr., "Saturation and inverse-saturation absorption line shapes in alexandrite," *J. Opt. Soc. Amer. B*, vol. 1, pp. 73–75, 1984.

[10] F. Y. Wu, S. Ezekiel, M. Ducloy, and B. R. Mollow, "Observation of amplification in a strongly driven two-level atomic system at optical frequencies," *Phys. Rev. Lett.*, vol. 38, pp. 1077–1080, 1977.

[11] M. T. Gruneisen, K. R. MacDonald, and R. W. Boyd, "Induced gain and modified absorption of a weak probe beam in a strongly driven sodium vapor," *J. Opt. Soc. Amer. B*, vol. 5, pp. 123–129, 1988.

[12] R. Gush and H. P. Gush, "Scattering of intense light by a two-level system," *Phys. Rev. A*, vol. 6, pp. 129–140, 1972.

[13] N. Tsukada, "Saturation effects of a two-level system in two rf fields," *J. Phys. Soc. Japan.*, vol. 46, pp. 1280–1287, 1979.

[14] A. M. Bonch-Bruevich, T. A. Vartanyan, and N. A. Chigir, "Subradiative structure in the absorption spectrum of a two-level system in a biharmonic radiation field," *Sov. Phys.—JETP*, vol. 50, pp. 901–906, 1979.

[15] N. Tsukada and T. Nakayama, "Modulation of optical bistability by an additional laser beam," *Phys. Rev. A*, vol. 25, pp. 964–977, 1982.

[16] G. I. Toptygina and E. E. Fradkin, "Theory of subradiative absorption structure in the interaction between two intense waves in a nonlinear medium," *Sov. Phys.—JETP*, vol. 55, pp. 246–251, 1982.

[17] G. S. Agarwal and N. Nayak, "Multiphoton processes in two-level atoms in two intense pump beams," *J. Opt. Soc. Amer. B*, vol. 1, pp. 164–168, 1984.

[18] L. W. Hillman, J. Krasinski, K. Koch, and C. R. Stroud, Jr., "Dynamics of homogeneously broadened lasers: Higher-order bichromatic states of operation," *J. Opt. Soc. Amer. B*, vol. 2, pp. 211–217, 1985.

[19] S. Chakmakjian, K. Koch, and C. R. Stroud, Jr., "Observation of resonances at sub-harmonics of the Rabi frequency in the saturated absorption of a 100% amplitude modulated laser beam," *J. Opt. Soc. Amer. B*, vol. 5, pp. 2015–2020, 1988.

[20] See, for example, J. C. Walling, O. G. Peterson, H. P. Jenssen, R. C. Morris, and E. W. O'Dell, "Tunable alexandrite lasers," *IEEE J. Quantum Electron.*, vol. QE-16, pp. 1302–1314, 1980.

[21] V. L. Vinetskii, N. V. Kukhtarev, S. G. Odulov, and M. S. Soskin, "Dynamic self-diffraction of coherent light beams," *Sov. Phys. Usp.*, vol. 22, pp. 742, 1979.

[22] M. Sargent III, M. O. Scully, and W. E. Lamb, *Laser Physics*. Reading, MA: Addison-Wesley, 1974, Sec. 7-3.

Mark T. Gruneisen was born in Gouverneur, NY, on May 15, 1958. He received the B.A. degree in physics and mathematics from the State University of New York College at Potsdam in 1980, and the M.S. and Ph.D. degrees in optics from the University of Rochester, Rochester, NY, in 1982 and 1988, respectively. His dissertation work involved the study of two-beam coupling and phase conjugation by resonant nonlinear optical interactions.

In 1989 he joined the Nonlinear Optics Center of Technology at the U.S. Air Force Weapons Laboratory, Kirtland AFB, NM. His current research interests center on mutually incoherent beam coupling and laser phase locking.

Previously, Dr. Gruneisen was a U.R.I. Fellow.

Kenneth R. MacDonald was born in Stoneham, MA, on August 5, 1955. He received the B.S. degree in chemistry and physics from Worcester Polytechnic Institute, Worcester, MA, in 1978, and the Ph.D. degree in physics from the University of Southern California, Los Angeles, in 1986. The topics of his doctoral research were photorefractive nonlinearities and the bulk photovoltaic effect.

From 1986 to 1988, he was a research associate with the Institute of Optics, University of Rochester, Rochester, NY, where he was involved in research on optical parametric nonlinearities, phase conjugation, and image processing. Since 1988, he has been a member of the technical staff with Rockwell Power Systems Company, Albuquerque, NM, where his scientific endeavors fall under the classifications of image processing and restoration, holographic optical systems, and techniques for phase-locking semiconductor lasers.

Dr. MacDonald is a member of Tau Beta Pi, the Optical Society of America, Sigma Xi, and Phi Lambda Upsilon.

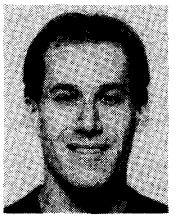

Alexander L. Gaeta was born in Halifax, N.S., Canada, in 1961. He received the B.S., M.S., and Ph.D. degrees in optics from the University of Rochester, Rochester, NY, in 1983, 1985, and 1990, respectively.

He currently holds a postdoctoral position with the Institute of Optics, University of Rochester. His research interests include instabilities and chaos in nonlinear optics, optical phase conjugation, stimulated scattering, and quantum-statistical properties of nonlinear optical processes.

Dr. Gaeta is a member of the Optical Society of America.

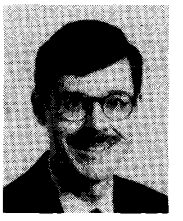

Robert W. Boyd (M'87) received the B.S. degree in physics in 1969 from the Massachusetts Institute of Technology, Cambridge, and the Ph.D. degree in physics in 1977 from the University of California, Berkeley. His dissertation work involved the use of nonlinear optical techniques for infrared detection for astronomy.

He joined the faculty of the Institute of Optics, University of Rochester, Rochester, NY, in 1977 and since 1987 has held the position of Professor of Optics. His research interests include studies of the nonlinear optical properties of materials, nonlinear optical interactions in atomic vapors, optical phase conjugation, and the development of new laser systems.

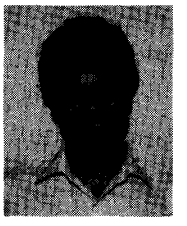

Donald J. Harter was born in Dearborn, MI, on November 2, 1951. He received the B.S.M.E. degree from Rensselaer Polytechnic Institute, Troy, NY, in 1973, the M.S.M.E. degree from Stanford University, Stanford, CA, in 1974, and the Ph.D. degree from the University of Rochester, Rochester, NY, in 1982. His dissertation topic was four-wave mixing enhanced by the ac Stark effect.

In 1974 he joined Inficon Incorporated to develop a nitrogen-pumped dye laser. In 1976 he began his Ph.D. studies at the Institute of Optics, University of Rochester. He is currently a Laser Physicist at Allied-Signal, Inc., Morristown, NJ, where he is primarily involved with alexandrite lasers. His research interests include laser physics and nonlinear optics.

Dr. Harter is a member of the Optical Society of America.